Proc. Natl. Acad. Sci. USA
Vol. 91, pp. 2081–2085, March 1994
Medical Sciences

Noninvasive measurement of microvascular and interstitial oxygen profiles in a human tumor in SCID mice

IVO P. TORRES FILHO*, MICHAEL LEUNIG†, FAN YUAN†, MARCOS INTAGLIETTA*, AND RAKESH K. JAIN†

*Institute for Biomedical Engineering, Department of Applied Mechanics and Engineering Sciences, University of California, San Diego, La Jolla, CA 92093; and †Steele Laboratory, Department of Radiation Oncology, Massachusetts General Hospital, Harvard Medical School, Boston, MA 02114

Communicated by Y. C. Fung, November 12, 1993 (received for review June 3, 1993)

ABSTRACT **Simultaneous measurements of intravascular and interstitial oxygen partial pressure (Po_2) in any tissue have not previously been reported, despite the importance of oxygen in health and in disease. This is due to the limitations of current techniques, both invasive and noninvasive. We have optically measured microscopic profiles of Po_2 with high spatial resolution in subcutaneous tissue and transplanted tumors in mice by combining an oxygen-dependent phosphorescence quenching method and a transparent tissue preparation. The strengths of our approach include the ability to follow Po_2 in the same location for several weeks and to relate these measurements to local blood flow and vascular architecture. Our results show that (*i*) Po_2 values in blood vessels in well-vascularized regions of a human colon adenocarcinoma xenograft are comparable to those in surrounding arterioles and venules, (*ii*) carbogen (95% O_2/5% CO_2) breathing increases microvascular Po_2 in tumors, and (*iii*) in unanesthetized and anesthetized mice Po_2 drops to hypoxic values at <200 μm from isolated vessels but drops by <5 mmHg (1 mmHg = 133 Pa) in highly vascularized tumor regions. Our method should permit noninvasive evaluations of oxygen-modifying agents and offer further mechanistic information about tumor pathophysiology in tissue preparations where the surface of the tissue can be observed.**

Oxygen is an important determinant of tumor growth and response to various therapies—e.g., radiation therapy, chemotherapy, and photodynamic therapy (1–3). This key role of oxygen has led to numerous theoretical and experimental investigations of oxygen partial pressure (Po_2) in rodent and human tumors. Most data on tissue Po_2 have been obtained by direct measurements using oxygen-sensing electrodes (1–12). Although such measurements are useful, there are several problems associated with them. (*i*) Electrodes are invasive and therefore may require the use of anesthetics. (*ii*) Po_2 is measured only along the electrode track, thus limiting the volume of tissue sampled. (*iii*) Repeated measurements in the same location in an unperturbed state over a long time period (several weeks) to study the effect of modifiers of oxygenation are not possible. (*iv*) The distances between the electrode tip and nearby blood vessels are not generally known. Indirect methods based on the detection of an oxygen-sensitive chemical probe by nuclear magnetic resonance, positron emission tomography, or electron paramagnetic resonance may overcome some of these problems, but these noninvasive methods do not have the spatial resolution to measure microvascular and interstitial Po_2 gradients (13–16). Quantitative autoradiography of tissues after injection of hypoxia-sensitive probes can provide the required spatial resolution, but this method is invasive and hence does not permit longitudinal studies in the same tumor.

Wilson and coworkers (17–19) recently pioneered a phosphorescence technique and obtained macroscopic, two-dimensional images (12,000 μm × 8000 μm) of Po_2 in normal and tumor tissue of anesthetized animals. We have used this technique to obtain Po_2 values in single microvessels and the interstitial Po_2 distribution at known distances from blood vessels with higher spatial resolution (≈15 μm). The Po_2 value decreases with distance from a capillary due to diffusion and/or perfusion limitation for a fixed rate of oxygen consumption. The only tumor measurements in the literature where this distance is known are due to Dewhirst *et al.* (20). However, their microelectrode technique was invasive, and their tumor preparation required superfusing the tissue. Moreover, it did not permit simultaneous intravascular Po_2 measurements.

We report here a noninvasive microscopic approach based on a modified Algire chamber preparation in severe combined immunodeficient (SCID) mice (21) and oxygen-dependent phosphorescence quenching (17–19, 43) to measure Po_2 in the microvascular and interstitial space of a human tumor xenograft. Blood flow and Po_2 were measured with and without anesthesia in animals breathing air or carbogen.

MATERIALS AND METHODS

Tumor Preparation. Dorsal skin chambers were implanted in SCID mice (Fig. 1) (21). This preparation allows one to monitor continuously and noninvasively microvessels and interstitium of subcutaneous skin tissue and transplanted tumors for up to 1 month. It also allows the simultaneous measurements of blood flow and Po_2 in microvessels as small as capillaries. Individual microcirculatory measurements were performed in five normal and six tumor-bearing chambers. Human colon adenocarcinoma LS174T was grown in the chamber for 14–18 days, until it reached a diameter of 4–6 mm.

***In Vivo* Microscopy.** Observations of the microcirculation were performed under an inverted microscope (IMT-2, Olympus, New Hyde Park, NY) using a ×20 objective and brightfield transillumination (halogen lamp, 12 V, 100 W). Images detected by a television camera (model 4815, Cohu, San Diego) were displayed on a television monitor (PVM-1342Q, Trinitron; Sony, Tokyo) and recorded on a video cassette recorder (AG-6500; Panasonic, Secaucus, NJ). Analysis of erythrocyte velocities and vessel diameters was performed off-line by means of a modified four-slit videophotometric technique (Microflow System, model 208C, video photometer version; IPM, San Diego) and an image shearing monitor (digital image shearing monitor, model 908; IPM). The blood flow rate was calculated as described by Leunig *et al.* (21). We did not classify tumor vessels as arteriolar or venular, since such a classification is not applicable to tumors (22, 23).

Oxygen Measurement. For Po_2 measurements, albumin-bound palladium (Pd)-coproporphyrin compound (Porphyrin Products, Logan, UT) was injected (13 mg/ml; 0.05 ml intravenously every 2 hr) into the bloodstream of the animal. Binding of the Pd-coproporphyrin to albumin increases its

The publication costs of this article were defrayed in part by page charge payment. This article must therefore be hereby marked "*advertisement*" in accordance with 18 U.S.C. §1734 solely to indicate this fact.

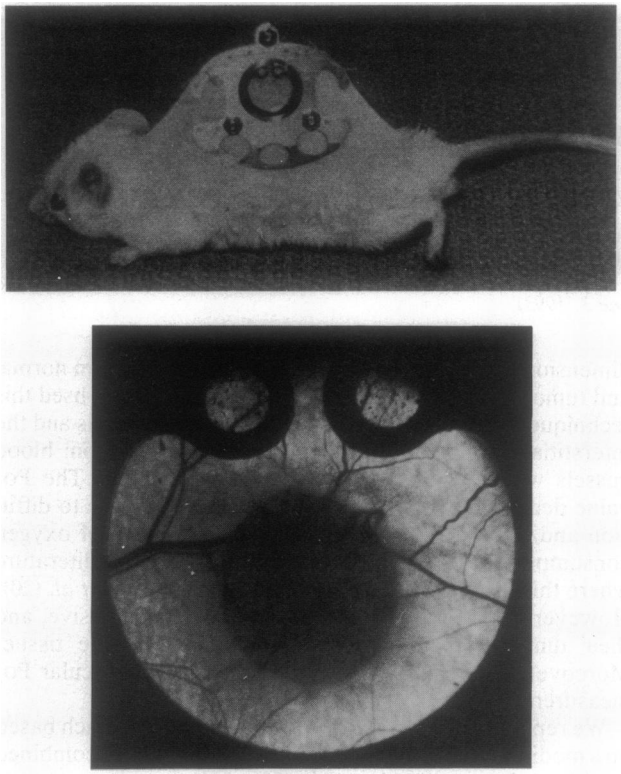

FIG. 1. (*Upper*) Dorsal skin-fold chamber in SCID mice was used to visualize microvessels in the subcutaneous tissue and in human colon adenocarcinoma LS174T transplanted into this preparation. The titanium chamber sandwiches a double layer of extended dorsal skin containing the microcirculatory preparation. (*Lower*) Transillumination photograph of an LS174T tumor (diameter, 5 mm) localized in the center of the chamber preparation, 14 days after tumor-cell implantation.

plasma half-life. Since blood vessels of tumor periphery are leaky (24–27), this compound readily extravasates into the interstitium and reaches uniform concentrations in <15 min, thus permitting vascular and interstitial Po_2 measurements. The tissue region of interest was excited with a flashlamp (decay constant, 10 μsec; frequency, 30 Hz; peak wavelength, 420 nm) (EG & G, Salem, MA) and phosphorescence signals from the superficial tissue layer were detected (630-nm cutoff filter). Depth of phosphorescence signal collection throughout the tissue was ≈10 μm for the ×20 dry objective (×20, SPlan, Olympus, Tokyo) used for all measurements, as determined *in vivo* by focusing and defocusing the region of interest. Only in exactly focused areas could phosphorescence signals be detected by the photomultiplier. The measuring "window" was 100 μm parallel and 15 μm perpendicular to the vessel wall. Both the lifetime (τ) and intensity of the emitted phosphorescence are dependent on oxygen concentration and can be used to measure Po_2; however, lifetime measurements are superior because they are independent of the local probe concentration and light intensity. The decay of the emitted phosphorescence following the excitation was monitored as a function of time by means of a photomultiplier tube (model 9855B, Thorn EMI Electron Tubes, Rockaway, NJ), digitized by an oscilloscope (model 2434, Tektronix), and stored on a microcomputer (43).

The phosphorescence lifetime (τ) was calculated and converted into Po_2 according to the Stern–Volmer equation:

$$Po_2 = \frac{1}{k}\left(\frac{1}{\tau} - \frac{1}{\tau_0}\right),$$

where k is the quenching constant and τ_0 is the value of τ at zero Po_2. Both constants (τ_0 and k) are dependent on pH and temperature, but for the albumin-bound Pd-coproporphyrin the pH dependence is negligible in the range 6.8–7.6 as

Table 1. Po_2, erythrocyte velocity (V), vessel diameter (D), and blood flow rate (Q) under various experimental conditions

Vessel	Condition	Po_2, mmHg	V, mm/sec	D, μm	Q, 10^{-6} ml/sec	Linear correlation, r*		
						Po_2/V	Po_2/D	Po_2/Q
Tumor vessels (N = 6)	Ua	29.9 ± 11.3 (27) (7.8–60.4)	0.21 ± 0.09 (24) (0.05–0.34)	37.8 ± 29.5 (27) (9.2–148.5)	133.2 ± 171.8 (24) (2.1–770.7)	0.068	0.489	0.116
	Uc	45.1 ± 21.5 (27) (6.7–117.0)	0.22 ± 0.12 (25) (0.06–0.55)	36.5 ± 29.3 (27) (14.4–148.5)	131.7 ± 178.1 (25) (8.1–805.8)	0.294	0.492	−0.038
	Aa	16.4 ± 7.8 (27) (3.6–33.7)	0.21 ± 0.16 (25) (0.04–0.66)	32.0 ± 27.6 (27) (12.5–138.2)	95.4 ± 137.9 (25) (6.9–502.9)	0.508	0.231	0.116
	Ac	40.6 ± 21.8 (27) (3.3–80.8)	0.19 ± 0.13 (24) (0.00–0.47)	32.7 ± 26.8 (27) (10.2–133.1)	108.8 ± 158.4 (24) (0.0–579.1)	0.675	−0.008	0.044
Arterioles (N = 5)	Ua	26.4 ± 9.5 (14) (15.7–46.2)	(>1.2)	34.7 ± 30.0 (14) (7.7–116.5)	—	—	0.271	—
	Uc	49.5 ± 22.4 (12) (20.0–91.7)	(>1.2)	34.4 ± 31.5 (14) (8.9–126.7)	—	—	0.115	—
	Aa	17.7 ± 6.1 (14) (11.3–31.3)	(>1.2)	34.4 ± 29.6 (14) (9.9–124.6)	—	—	−0.115	—
	Ac	31.0 ± 18.5 (14) (13.0–62.1)	(>1.2)	32.7 ± 30.1 (11) (7.7–106.2)	—	—	0.381	—
Venules (N = 5)	Ua	25.3 ± 5.6 (43) (16.5–37.2)	0.30 ± 0.13 (35) (0.09–0.74)	38.4 ± 24.7 (43) (6.5–128.7)	319.7 ± 428.5 (35) (3.4–2032.0)	0.083	0.107	0.126
	Uc	36.0 ± 10.9 (42) (17.7–57.8)	0.28 ± 0.09 (35) (0.06–0.53)	38.7 ± 22.5 (43) (12.9–132.4)	281.8 ± 468.5 (35) (6.6–2753.0)	−0.081	0.032	0.038
	Aa	15.7 ± 4.2 (40) (7.4–29.2)	0.29 ± 0.11 (35) (0.00–0.54)	36.3 ± 21.6 (39) (13.6–120.0)	299.9 ± 544.3 (35) (0.0–2755.0)	0.010	−0.099	−0.144
	Ac	20.6 ± 10.5 (40) (11.5–57.2)	0.25 ± 0.10 (36) (0.07–0.59)	37.4 ± 22.0 (40) (10.9–116.5)	233.0 ± 330.1 (36) (6.4–1731.0)	0.206	0.221	0.393

N, no. of animals; Ua, unanesthetized, air breathing; Uc, unanesthetized, carbogen breathing; Aa, anesthetized, air breathing; Ac, anesthetized, carbogen breathing. Values are mean ± SD with no. of measured vessels (n) and range of values in parentheses. Erythrocyte velocity of arterioles is >1.2 mm/sec and cannot be measured by our system. Thus, blood flow rate could not be calculated for arterioles.
*Pearson correlation coefficient.

determined *in vitro*. At 32°C and pH 7.0, the *in vitro* calibration gives k = 240 $mmHg^{-1}\cdot sec^{-1}$ and τ_0 = 940 μsec, respectively (1 mmHg = 133 Pa). Since the values of τ_0 and k are specific to the compound bound to albumin at a given pH and temperature, τ_0 and k determined *in vitro* hold for measurements *in vivo* (17–19). The uncertainty (ΔPo_2) of calculated Po_2 values depends on the errors in τ_0 and k,

$$\Delta Po_2 = Po_2 \frac{\Delta k}{k} + \frac{1}{k\tau_0}\frac{\Delta \tau_0}{\tau_0}.$$

In our study, the maximum value of $\Delta k/k$ or $\Delta\tau_0/\tau_0$ was <4%. Although the method provides sensitivity to oxygen over the whole physiological Po_2 range, the determinations are particularly accurate at low Po_2. For instance, in the range 0–5 mmHg, a ±15% error in the estimation of τ leads to a calculated Po_2 of less than ±1 mmHg, whereas at the level of 30 mmHg, the calculated Po_2 would change ±5 mmHg for the same variability in the estimation of τ.

Experimental Protocol. Erythrocyte velocity, vessel diameter, and Po_2 were measured in six tumor-bearing and five control animals. In each animal, at least eight intravascular or extravascular regions were studied. Each animal was studied both in the awake (U) and in the anesthetized condition (A; 7.5 mg of ketamine hydrochloride and 2.5 mg of xylazine per 100 g of body weight, subcutaneously), breathing either room air (a) or carbogen (c; 95% O_2/5% CO_2). The time sequence of the four different combinations of treatment (Ua, Aa, Uc, Ac) for each animal was randomly selected and the same region was studied under each treatment. Taken together, >100 different regions were studied, and >400 measurements were performed for each parameter. In spite of the variability of individual responses, the results were qualitatively similar for each animal studied. The temperature of the skin in the area under study was periodically measured with a thermocouple (Physitemp, Clifton, NJ). Individual skin temperatures were then used to calculate the appropriate values of τ_0 and k for every animal under each experimental situation.

Data groups were statistically compared by the least-mean-square method, and linear correlations were tested with the Pearson correlation coefficient.

RESULTS AND DISCUSSION

Due to the invasive nature of the currently used approaches, almost all Po_2 data have been obtained in anesthetized animals. Our approach enabled us to compare blood flow and Po_2 in awake and in anesthetized animals. Table 1 shows Po_2, erythrocyte velocity, vessel internal diameter, and blood flow rate in individual vessels in awake and anesthetized animals. Table 2 gives the significance levels for Po_2 values under these conditions. Note that anesthesia did not significantly alter vessel diameter, erythrocyte velocity, or blood flow rate despite an ≈20% reduction in mean arterial pressure and an ≈35% decrease in heart rate in these mice (21). Intravascular Po_2, however, significantly decreased in normal arterioles and venules and in tumor vessels, probably due to a reduction (22%) in breathing rate (Fig. 2). Our Po_2 values in arterioles are comparable to reported values (28–31).

Table 2. Significance levels for Po_2 values as tested by the least-mean-square method

Vessel		Uc	Aa	Ac
Tumor vessels	Ua	0.0091	0.1843	0.2339
	Uc		0.0002	0.1375
	Aa			0.0149
Arterioles	Ua	0.0004	0.0001	0.0245
	Uc		0.0001	0.1909
	Aa			0.0001
Venules	Ua	0.0001	0.0001	0.0001
	Uc		0.0001	0.0001
	Aa			0.0001

Ua, unanesthetized, air breathing; Uc, unanesthetized, carbogen breathing; Aa, anesthetized, air breathing; Ac, anesthetized, carbogen breathing.

Various studies in the literature have suggested that human tumors have a higher Po_2 and/or hemoglobin oxygen saturation compared with rodent tumors (1–16). Our results on the effect of anesthesia on Po_2 offer a possible explanation for these differences. Most human Po_2 studies were conducted in unanesthetized patients, whereas animal studies were usually done under anesthesia. These differences may become even larger if anesthesia decreases the tumor blood flow rate in addition to suppressing breathing rate.

We did not find a statistically significant difference in Po_2 between normal and tumor vessels (Table 1). This does not exclude the possibility that the blood vessels in the deeper region of our tumor model may be less oxygenated than in the periphery. However, our method permits measurements only at the tumor surface. This differs from results of Wilson and Cerniglia (17), who reported that 9L glioma vessels have a lower Po_2 than that in the surrounding normal tissue in anesthetized animals. In their study, macroscopic phosphorescence measurements in tumors contained signals from intravascular and interstitial spaces due to "leaky" structure

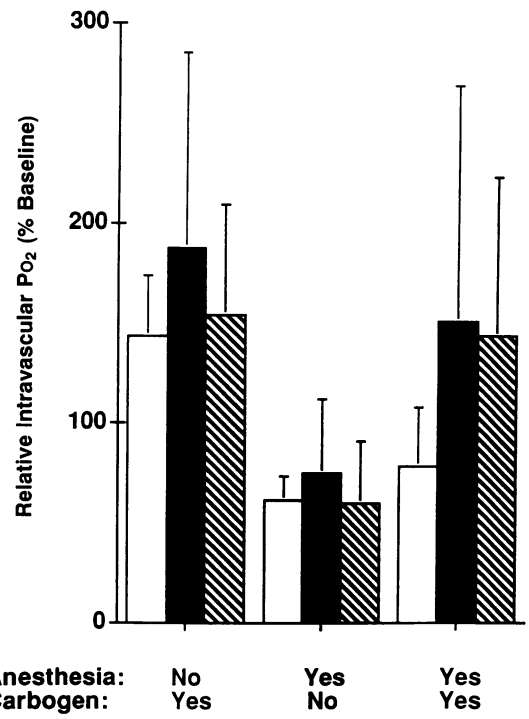

FIG. 2. Mean and standard deviation of relative Po_2 values of three (sequential) measurements in the venules [no. of animals (N) = 5, no. of measurements (n) = 40] (open bars) and arterioles (N = 5, n = 12) (filled bars) of the subcutaneous tissue of the dorsal skin-fold chamber and in blood vessels (N = 6, n = 27) of the LS174T human adenocarcinoma (hatched bars) implanted into the dorsal skin chamber preparation (mean vessel diameter, 35 μm). The Po_2 level of the awake animal breathing air was taken as the baseline (see Table 1). Under these experimental conditions no significant differences of Po_2 values between subcutaneous tissue venules and arterioles and the tumor blood vessels were found. In all vessels, carbogen breathing increased Po_2 in unanesthetized mice. Anesthesia in animals breathing normal room air decreased local Po_2, whereas carbogen breathing of anesthetized mice again increased Po_2 in venules, arterioles, and tumor blood vessels. (For statistical significance, see Table 2.)

of tumor vessels (see below) whereas normal tissue measurements were based on intravascular signals. Since interstitial Po_2 is less than microvascular Po_2, it is likely that those tumor Po_2 values were a weighted average of intra- and extravascular values.

Most preparations used in microvascular research rely on the direct visualization of the microvessels, and the technique should be applicable in most circumstances. Our system extends the range of applicability of the phosphorescence technique and allowed Po_2 determinations in areas at least 3 orders of magnitude smaller than previously reported. In addition, the system allowed measurement of other microcirculatory parameters, such as microvessel diameter and blood flow, at the same location (43). The contribution from areas below the vessel under study was probably small because the emission from those regions is strongly absorbed by the intravascular blood column.

Several agents have been used to increase tumor Po_2 to enhance the outcome of radiation therapy (2, 3). One method is to use carbogen breathing (32). As shown in Fig. 2, carbogen breathing increased vascular Po_2 in both unanesthetized and anesthetized mice.

Leakage of the albumin-bound porphyrin out of the blood pool in vessels at the tumor periphery (24–27) enabled us additionally to measure Po_2 in interstitial regions of LS174T tumors. We measured Po_2 profiles around single vessels up to a distance of ≈350 μm from the vessel wall in poorly vascularized regions and between two parallel vessels, ≈100 μm apart in well-vascularized regions, with a resolution of 15 μm perpendicular to the blood vessel. A total of 11 gradients

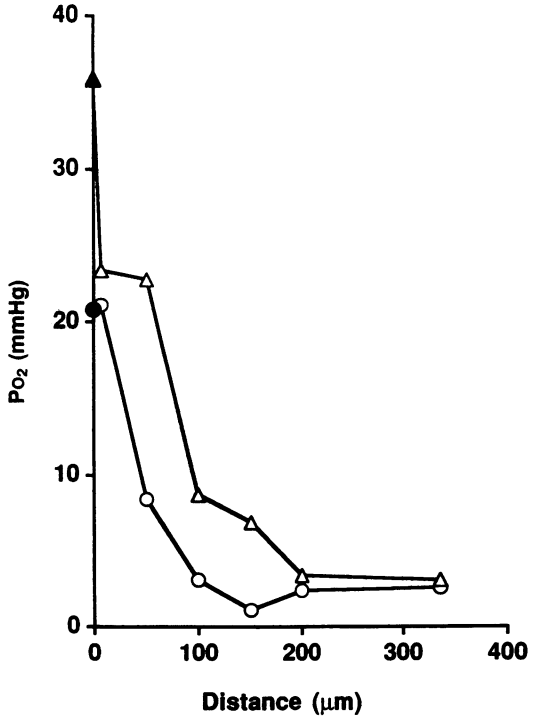

FIG. 3. Data from one Po_2 gradient obtained from measurements in the intravascular and in the interstitial space of an LS174T tumor of a SCID mouse under unanesthetized (triangles) and anesthetized (circles) conditions. The Po_2 dropped exponentially and reached plateau values of ≈3 mmHg at around 200 μm away from the blood vessel. The filled symbols represent the Po_2 in the vessel (at 0 μm). The drop of local Po_2 in the interstitial space away from a single vessel was more pronounced when compared with that between two blood vessels (see Fig. 4). In tumors of anesthetized mice, plateau values were slightly lower than in tumors of unanesthetized mice; however, due to a reduced intravascular Po_2, the drop was less pronounced.

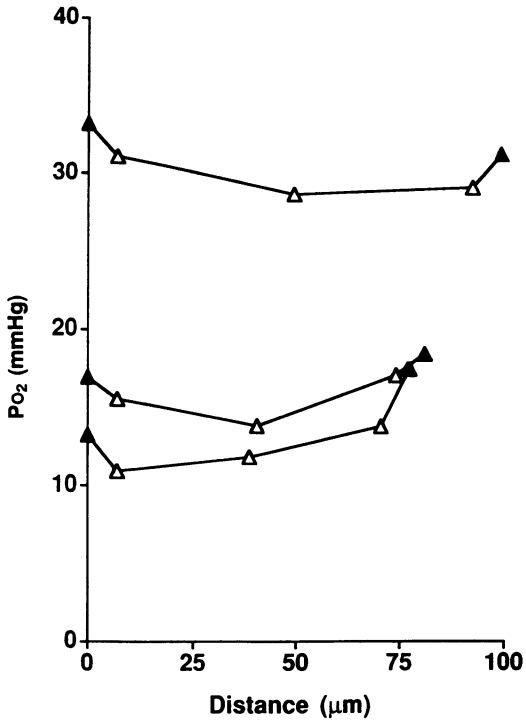

FIG. 4. Data from three Po_2 profiles in the interstitial space (open triangles) between two tumor blood vessels (filled triangles) in unanesthetized mice breathing room air. The distance between both vessels for all three LS174T tumors grown in dorsal chamber in SCID mice was <100 μm. Maximum drop in Po_2 from these vessels to the interstitium was 4 mmHg.

were determined, all showing the same trend. Figs. 3 and 4 present examples of individual Po_2 profiles. Note that the interstitial Po_2 values are smaller than and depend strongly on the intravascular Po_2 of the nearby blood vessels. Large variations among intravascular Po_2 in tumors led to large differences in interstitial Po_2. In our chamber preparation, vessels are accessible only at the tumor surface, where vessel density is highest. In the rare cases when we found intervessel distances of >200 μm, Po_2 dropped to hypoxic values at ≈200 μm, which corresponds to observations and calculations previously reported (33–39). On the other hand, the slight Po_2 drop between two parallel vessels <100 μm apart was less than that calculated from a single isolated Krogh cylinder analysis (33–39). However, when one considers the interaction between vessels, this slight drop is not surprising (33–39).

In conclusion, we have presented intravascular and interstitial measurements of Po_2. Although our approach has certain limitations and cannot replace invasive as well as noninvasive methods currently used in the clinic, it will permit the testing of hypotheses on tissue oxygenation and the evaluation of oxygen-modifying agents, and it will offer further mechanistic information about tumor pathophysiology (40–42).

We wish to express our gratitude to J. Efird for his help in the statistical analysis; P. C. Johnson, R. Shonat, and W. Tompkins for their help with instrumentation; and D. A. Berk, J. Biaglow, J. M. Brown, M. W. Dewhirst, B. Duling, L. Gerweck, P. M. Gullino, I. Lee, K. Messmer, J. S. Rasey, C. W. Song, H. Stone, H. D. Suit, P. Vaupel, and D. F. Wilson for their critical and helpful comments. This work was supported by National Institutes of Health Grants CA37239 and HL17421. I.P.T.F. is a previous recipient of Fogarty International Center and Brazilian Research Council Fellowships, and is currently supported by The Pew Charitable Trusts and Universidade do Estado do Rio de Janeiro. M.L. is a recipient of a Feodor Lynen Fellowship of the Humboldt Foundation.

1. Sutherland, R. M. (1988) *Science* **240,** 177–184.
2. Vaupel, P. & Jain, R. K., eds. (1991) *Tumor Blood Supply and Metabolic Microenvironment* (Fischer, Stuttgart, Germany).
3. Teicher, B., ed. (1993) *Drug Resistance in Oncology* (Dekker, New York).
4. Urbach, F. (1956) *Proc. Am. Assoc. Cancer Res.* **2,** 154–155.
5. Cater, D. B. & Silver, I. A. (1960) *Acta Radiol.* **53,** 233–256.
6. Evans, N. T. S. & Naylor, P. F. D. (1963) *Br. J. Radiol.* **36,** 418–425.
7. Kolstad, P. K. (1964) *Norwegian Monograph on Medical Science* (Universitetsforlaget, Oslo).
8. Jamieson, D. & van den Brenk, H. A. S. (1965) *Br. J. Cancer* **19,** 139–150.
9. Gullino, P. M. (1970) *Methods Cancer Res.* **5,** 45–91.
10. Vaupel, P. (1977) *Microvasc. Res.* **13,** 399–408.
11. Gatenby, R. A., Kessler, H. B., Rosenblum, J. S., Coia, L. R., Moldofsky, P. J., Hartz, W. H. & Broder, G. J. (1988) *Int. J. Radiat. Oncol. Biol. Phys.* **14,** 831–838.
12. Höckel, M., Schlenger, K., Knoop, C. & Vaupel, P. (1991) *Cancer Res.* **51,** 6098–6102.
13. Rasey, J. S., Koh, W. J., Grierson, J. R., Grunbaum, Z. & Krohn, K. A. (1989) *Int. J. Radiat. Oncol. Biol. Phys.* **17,** 985–991.
14. Chapman, J. D. (1991) *Radiother. Oncol.* **20,** Suppl., 13–19.
15. Swartz, H. M., Boyer, S., Gast, P., Glockner, J. F., Hu, H., Liu, K. J., Moussavi, M., Norby, S. W., Vahidi, N., Walczak, T., Wu, M. & Clarkson, R. B. (1991) *Magn. Reson. Med.* **20,** 333–339.
16. Kwock, L., Gill, M., McMurry, H. L., Beckman, W., Raleigh, J. A. & Joseph, A. P. (1992) *Radiat. Res.* **129,** 71–78.
17. Wilson, D. F. & Cerniglia, G. J. (1992) *Cancer Res.* **52,** 3988–3993.
18. Rumsey, W. L., Vanderkooi, J. M. & Wilson, D. F. (1988) *Science* **241,** 1649–1651.
19. Wilson, D. F., Pastuszko, A., DiGiacomo, J. E., Pawlowski, M., Schneiderman, R. & Delivoria-Papadopoulos, M. (1991) *J. Appl. Physiol.* **70,** 2691–2696.
20. Dewhirst, M. W., Ong, E. T., Klitzman, B., Secomb, T. W., Vinuva, R. Z., Dodge, R., Brizel, D. & Gross, J. F. (1992) *Radiat. Res.* **130,** 171–182.
21. Leunig, M., Yuan, F., Menger, M. D., Boucher, Y., Goetz, A. E., Messmer, K. & Jain, R. K. (1992) *Cancer Res.* **52,** 6553–6560.
22. Eddy, H. A. & Cassarett, G. W. (1973) *Microvasc. Res.* **6,** 63–82.
23. Jain, R. K. (1988) *Cancer Res.* **48,** 2641–2658.
24. Gerlowski, L. E. & Jain, R. K. (1986) *Microvasc. Res.* **31,** 288–305.
25. Jain, R. K. (1987) *Cancer Metastasis Rev.* **6,** 559–593.
26. Baxter, L. T. & Jain, R. K. (1989) *Microvasc. Res.* **37,** 77–104.
27. Yuan, F., Leunig, M., Berk, D. A. & Jain, R. K. (1993) *Microvasc. Res.* **45,** 269–289.
28. Duling, B. R. & Berne, R. M. (1970) *Circ. Res.* **27,** 669–678.
29. Duling, B. R. (1973) *Circ. Res.* **32,** 370–376.
30. Duling, B. R., Kuschinsky, W. & Wahl, M. (1979) *Pflügers Arch.* **383,** 29–34.
31. Weerappuli, D. P., Pittman, R. N. & Popel, S. A. (1990) *J. Theor. Biol.* **147,** 275–288.
32. Falk, S. J., Ward, R. & Bleehen, N. M. (1992) *Br. J. Cancer* **66,** 919–924.
33. Krogh, A. (1919) *J. Physiol. (London)* **52,** 409–415.
34. Thomlinson, R. H. & Gray, L. H. (1955) *Br. J. Cancer* **9,** 539–549.
35. Tannock, I. F. (1972) *Br. J. Radiol.* **45,** 515–524.
36. Kreutzer, F. (1982) *Experientia* **38,** 1415–1426.
37. Degner, F. L. & Sutherland, R. M. (1988) *Int. J. Radiat. Oncol. Biol. Phys.* **15,** 391–397.
38. Groebe, K. & Vaupel, P. (1988) *Int. J. Radiat. Oncol. Biol. Phys.* **15,** 691–697.
39. Secomb, T. W., Hsu, R., Dewhirst, M. W., Klitzman, B. & Gross, J. F. (1993) *Int. J. Radiat. Oncol. Biol. Phys.* **25,** 481–489.
40. Folkman, J. (1985) *Adv. Cancer Res.* **43,** 175–203.
41. Coleman, C. N. (1988) *J. Natl. Cancer Inst.* **80,** 310–317.
42. Eskey, C. J., Koretsky, A. P., Domach, M. M. & Jain, R. K. (1993) *Proc. Natl. Acad. Sci. USA* **90,** 2646–2650.
43. Torres Filho, I. P. & Intaglietta, M. (1993) *Am. J. Physiol. Suppl.* **265,** H1434–H1438.